

Combining Structure Modeling and Electron Microscopy to Determine Complex Zeolite Framework Structures**

Yi Li, Jihong Yu,* Ruren Xu, Christian Baerlocher, and Lynne B. McCusker

Zeolites are a family of open-framework aluminosilicates that are widely used in fields as diverse as catalysis, adsorption, and ion exchange. Although all zeolite frameworks consist of tetrahedrally coordinated atoms such as Si and Al (T atoms) bridged by O atoms, the different ways in which they can be connected lead to zeolite frameworks with wide structural diversity.^[1] To fully exploit their unusual functions and features, it is essential that their structures be understood on an atomic level. They are typically prepared under hydrothermal conditions and usually crystallize in polycrystalline form (crystallites with a volume of less than 100 μm^3), so conventional single-crystal methods of structure analysis cannot be applied. In the past decades, many zeolite structures have been solved by using X-ray powder diffraction techniques,^[2] high-resolution transmission electron microscopy (HRTEM) data,^[3–7] and, very recently, a combination of both.^[8,9] An alternative approach to zeolite structure determination is to use computer-assisted model building based on prior knowledge such as chemical composition, symmetry, coordination geometry, and connectivity.^[10–13]

The well-established T–O distances, O–T–O angles, and T–O–T angles are the fundamental constraints used in all structure-modeling procedures. However, with only the information on bonding geometry, complex zeolite structures, especially those with more than ten T atoms in the asymmetric unit, have proved to be difficult to solve by modeling, because of the computational overhead caused by the large number of degrees of freedom. One way to tackle this problem is to introduce additional, experimentally derived, structural information into the computational modeling procedure. It

seemed natural to concentrate on the porosity of a zeolite for this purpose, as that is the key structural difference between zeolites and other silicate framework materials.^[14–16] Furthermore, many studies have demonstrated that such information can easily be extracted from HRTEM images.

Here we present a Monte Carlo model-building method for determining the structures of complex zeolite frameworks. In contrast to other model-building procedures, this approach uses structural information derived from one or more HRTEM images as an additional constraint in the computational modeling procedure. A term that evaluates the agreement between the structure models generated and the HRTEM image has been added to the cost function for structure simulation. To the best of our knowledge, this is the first time that HRTEM images have been used directly in real-space Monte Carlo simulation. Our results show that by using just one HRTEM image as a constraint, the number of degrees of freedom for solving the structure-modeling problem can be reduced to a practically manageable level, even for the most complex zeolite structures. The power of this approach is demonstrated with the solutions of the structures of IM-5 ($[\text{Si}_{288}\text{O}_{576}]$) and TNU-9 ($[\text{Si}_{192}\text{O}_{384}]$), the two most complex zeolite structures known.

Zeolite IM-5 ($[\text{Si}_{288}\text{O}_{576}]$) was first synthesized in 1998,^[17] but its structure was not determined until 2007.^[9] The extremely large unit cell of IM-5 ($V > 16000 \text{ \AA}^3$) and the approximate relationships between the unit-cell axes cause severe problems with reflection overlap (over 80% of the reflection intensities are ambiguous). Furthermore, the asymmetric unit contains 24 topologically distinct T atoms, and this makes the IM-5 framework structure one of the two most complex known. The structure was finally solved by combining high-resolution X-ray powder diffraction data with HRTEM techniques in an enhanced charge-flipping algorithm.^[9]

In our structure-modeling approach, the quality of the X-ray or electron diffraction data is not crucial as long as the cell parameters and the possible space groups can be deduced. Even if these are ambiguous, simulations can be run separately for each possibility. As an ultimate test of our algorithm, we ran a simulation using the ideal unit cell of IM-5 (space group *Cmcm*, cell parameters: $a = 14.30$, $b = 56.79$, and $c = 20.29 \text{ \AA}$). As in all other structure-modeling methods, we defined a cost function based on the structural geometry of known zeolite frameworks, and used this function in conjunction with simulation algorithms to obtain an optimized structure. The total cost value E was calculated from the sum of several weighted terms describing the average T–T distance ($E_{\text{d(T-T)}}$), the average T–T–T angle ($E_{\text{a(T-T-T)}}$), and the connectivity (E_{conn}). In addition, we introduced the new term

[*] Dr. Y. Li, Prof. J. Yu, Prof. R. Xu
State Key Laboratory of Inorganic Synthesis and Preparative Chemistry
Jilin University, Changchun 130012 (China)
Fax: (+86) 431-85168608
E-mail: jihong@jlu.edu.cn

Dr. C. Baerlocher, Dr. L. B. McCusker
Laboratory of Crystallography, ETH Zurich
8093 Zurich (Switzerland)

[**] This work is supported by the National Natural Science Foundation of China, the State Basic Research Projects of China (2006CB806103 and 2007CB936402), and Major International (Regional) Joint Research Project. Y.L. thanks the Swiss State Secretariat for Education and Research for the scholarship that allowed him to work for nine months at the ETH in Zurich. We thank Prof. Xiaodong Zou and Prof. Osamu Terasaki at Stockholm University for providing the HRTEM images and valuable discussions. Thanks also to Prof. Ying Xu at the University of Georgia for his helpful suggestions.

Supporting information for this article is available on the WWW under <http://www.angewandte.org> or from the author.

E_{map} , which reflects the degree of agreement between the positions of the T atoms and the potential map derived from the HRTEM image.

For IM-5, the potential map was constructed from a symmetry-averaged HRTEM image along the [100] direction (Figure 1a), because this image was relatively easy to obtain.^[9] The channels along the [100] direction are easily

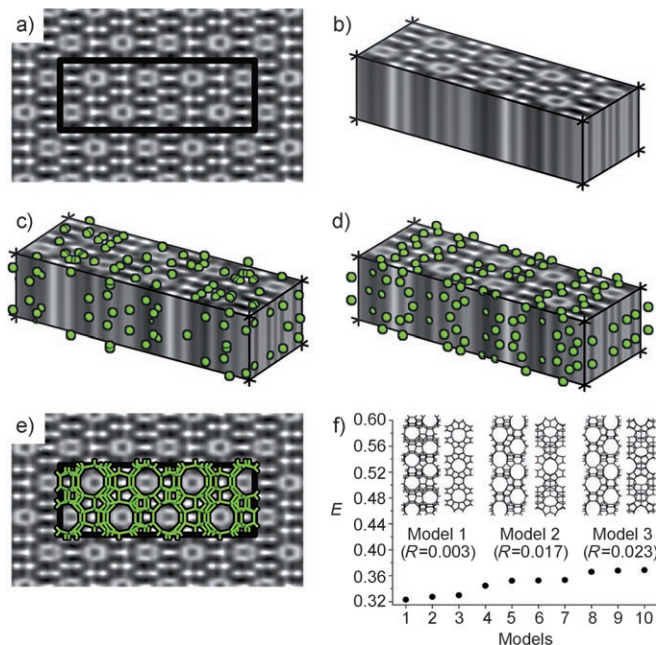


Figure 1. Generation of the IM-5 framework in a three-dimensional potential map derived from one HRTEM image along the [100] direction. a) The HRTEM image of IM-5 along the [100] direction. b) The potential map generated from the image shown in (a). c) T atoms placed randomly in the potential map at the beginning of the simulation. d) T atoms rearranged in the potential map during the simulation. e) Agreement between the generated structure model and HRTEM image along the [100] direction. f) Plot of the cost values of the generated structure models. All generated models are unique, and only the ten models with the lowest cost values are shown. Model 1 has the lowest cost value and the best R_{DLS} value, and it corresponds to the correct structure solution. Its framework projections along the [100] and [001] directions are displayed together with those of two other models with low cost values. Detailed information about the HRTEM images can be found in reference [9].

recognized. The gray scale gives an approximation of the potential projected along the [100] direction. This two-dimensional projection was then expanded over the whole unit cell (Figure 1b). In this way, each point in the unit cell is given a fixed potential value determined from its projection on the HRTEM image. Although this three-dimensional map is not physically real, it divides the unit cell into regions where atoms may be located and those where they may not. A threshold value for the potential is defined, and atoms in regions with values above this threshold do not contribute to the E_{map} term of the cost function, while those in the other regions contribute substantially.

At the beginning of each simulation, an estimated number of T atoms (based on the framework density) are introduced

into the asymmetric unit of the unit cell in a random fashion, and their equivalent atoms generated by symmetry operators. At this stage, the bonding geometry of the generated structure model may be unrealistic, and aggregates of T atoms may be observed (Figure 1c). During the simulation, a reasonable bonding geometry is sought by moving the T atoms around. More importantly, atoms are “pushed” from the low-potential area into the high-potential area to fit the potential map (Figure 1d). The cost function (and thereby the structure) is optimized by using a simulated annealing^[18] and parallel tempering algorithm.^[13] At each temperature stage, configuration-biased Monte Carlo^[13] is used for sampling. At the end of the simulation, the framework with the lowest cost value is saved. The bridging O atoms are added between the nearest T–T pairs, and the bonding geometry of the entire structure is further optimized by using a simple distance least-squares (DLS) algorithm.^[19] Coordination sequences^[20] are calculated for structure identification. Then a new simulation cycle is started by reassigning random coordinates to all atoms.

The simulation program FGDM (framework generation in density maps) is written in FORTRAN and was compiled on a desktop PC with an Intel Core 2 Duo processor. For IM-5, each simulation cycle took 2–20 min, depending on the sampling scheme. After 500 cycles, 250 distinct four-connected structure models were generated. All the generated models fit the HRTEM image along the [100] direction very well (Figure 1e). A plot of the cost values of all structures generated is shown in Figure S1 in the Supporting Information. A plot of the cost values for the ten best models along with the projections of the three frameworks with the lowest cost values is shown in Figure 1f. Of all the generated structures, Model 1 has the lowest cost value E and the best DLS reliability factor R_{DLS} . Comparison of the simulated and experimental X-ray diffraction patterns shows Model 1 to be the correct structure model for IM-5.

The efficiency of the structure solution could be improved by using a potential map generated from a better image. For IM-5, the image along the [001] direction (Figure 2a) was more difficult to get, but has better contrast than that along the [100] direction.^[9] By using this image, the correct structure solution of IM-5 could be found within 200 cycles (see Figure S2 in the Supporting Information) and has the lowest E and R_{DLS} values (Figure 2b). Considering the complexity of this structure and the limited information used (space group, cell parameters, number of T atoms, and a single HRTEM image), the efficiency of the approach is surprisingly high. We continued the investigation to see if the efficiency could be further improved by including additional constraints.

An obvious step was to use both of the HRTEM images (along the [100] and the [001] directions) together. Since the image along the [001] direction has much better contrast than the one along [100], we assigned weights of ten and one to the corresponding potential maps, respectively. During the simulation, only structures fitting both maps could yield low cost values. Using this procedure, approximately 15 correct solutions could be generated within 100 cycles. In this case, the correct solution was found more often than all other models. A histogram showing the frequency of occurrence for

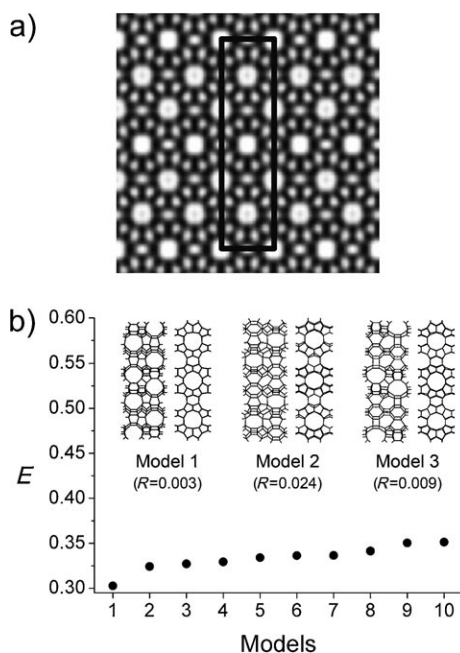


Figure 2. Generation of the IM-5 framework in a three-dimensional potential map derived from one HRTEM image along the [001] direction. a) The HRTEM image of IM-5 along the [001] direction. b) Plot of the cost values of the structure models generated by using the image shown in (a). Only the ten models with the lowest cost values are shown. Model 1 has the lowest cost value and the best R_{DLS} value, and it corresponds to the correct structure solution. Its framework projections along the [100] and [001] directions are displayed together with those of two other models with low cost values. Detailed information about the HRTEM images can be found in reference [9].

the different structure models generated with this approach is shown in Figure S3 in the Supporting Information. The correct structure model for IM-5 could be easily distinguished from the others. It has the lowest cost value and the highest frequency of occurrence.

In a further attempt to improve the computational efficiency, we also investigated the effect of introducing constraints on the movement of atoms. During the simulation, atoms were constrained to move around their initial positions. The initial placement of T atoms can be derived from the HRTEM image directly by using the shift-overlap multiply enhancement method (SOMEM) introduced by Ohsuna et al. in 2002.^[21] This procedure enhances the peaks in a potential map, so that approximate atomic positions can be retrieved from a blurred map.

Alternatively, approximate atomic coordinates for parts of the structure could be assigned manually, based on our general knowledge of zeolite frameworks. For IM-5, for example, a “butterfly” building block is readily apparent in the HRTEM image along the [001] direction (Figure 3a). This building block, which is common in siliceous zeolite frameworks,^[1] consists of four 5-rings and one 6-ring. Although it was not possible to get the precise coordinates of the atoms in the butterfly unit, values for x and y could be estimated. The z coordinates were then generated randomly.

During the simulation, atoms are allowed to move away from their initial positions to improve their bonding geo-

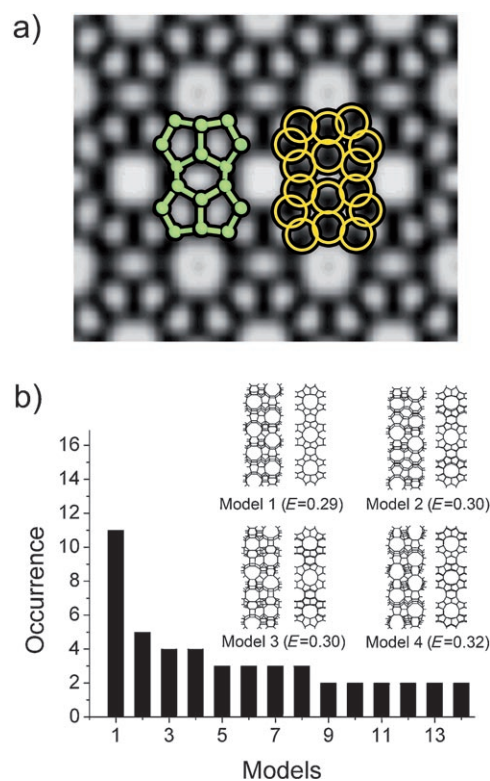


Figure 3. Generation of the IM-5 framework by using one HRTEM image along the [001] direction with constraints on the movement of atoms. a) Ball-and-stick model of the “butterfly” building block in IM-5 and the corresponding range of atomic positions allowed in the simulation (yellow circles). The radius of these circles (ca. 1.75 Å) has been significantly reduced for clarity. The background HRTEM image is along the [001] direction. b) Histogram showing the frequency of occurrence for the different structure models generated. Model 1, corresponding to the framework of IM-5, could easily be distinguished from others. It has the lowest cost value and occurs with the highest frequency. Its framework projections along the [100] and [001] directions are displayed above the histogram, together with those of three other models with low cost values and high frequencies of occurrence.

metries and connectivities. The maximum deviation allowed during the simulation is defined at the outset. For example, the centers of the yellow circles shown in Figure 3a are the initial atomic positions, and the radius of each circle is the maximum deviation allowed in the xy plane during the simulation. The radius of the circle can be adjusted according to the resolution of the HRTEM image and/or the flexibility of the unit involved. By setting the radius at 3.0 Å, about ten solutions were obtained within 100 cycles when just the image along the [001] direction was used, and about 50 solutions were found when the image along [100] was added. In both cases, the correct solution was found more often than all other models. Histograms showing the frequency of occurrence for the different structure models generated in these two runs are shown in Figure 3b and Figure S4 in the Supporting Information. As expected, more images with higher resolution accelerate the structure solution significantly.

To further test the algorithm, we also attempted to solve the structure of the zeolite TNU-9, which has a complexity similar to that of IM-5. This structure was also difficult to

solve by conventional powder diffraction methods, because of the severe reflection-overlap problem. It was originally solved by combining high-resolution powder diffraction data with HRTEM images in the zeolite-specific structure-solution algorithm FOCUS.^[8,22,23] With the program FGDM, the structure of TNU-9 could be solved easily by incorporating the pore information from the high-quality HRTEM image along the [010] direction.^[8] A plot of the lowest cost values found for the TNU-9 simulation, starting with random coordinates is shown in Figure 4a, and a histogram showing the frequency of occurrence of the different models generated with constraints on the movement of atoms around rational starting coordinates in Figure 4b.

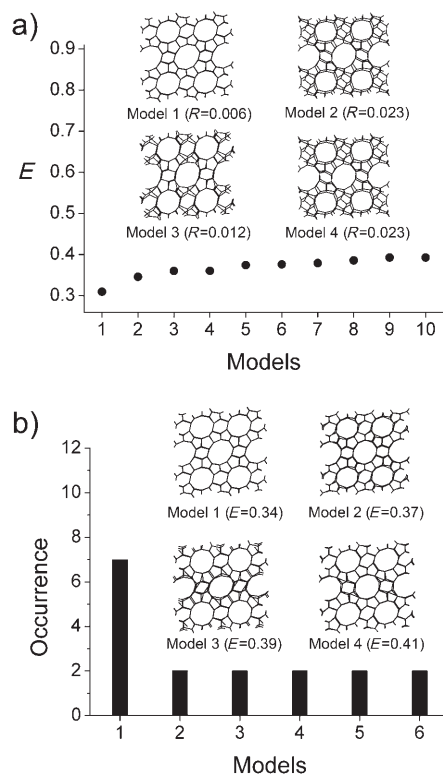


Figure 4. Structure models generated during the solution of the structure of TNU-9. a) Plot of the cost values of the structure models generated with random starting configurations. Only the ten models with the lowest cost values are shown. Model 1 has the lowest cost value and the best R_{DLS} value and it corresponds to the correct structure solution. Its framework projection along [010] is shown, together with those of three other models with low cost values. b) Histogram of the structure models generated with constraints on the movement of atoms. Only models occurring more than once are shown. Model 1, which corresponds to the TNU-9 framework, has the lowest cost value and the highest frequency of occurrence. Its framework projection along [010] is displayed together with those of three other models with low cost values.

The three-dimensional potential maps used for IM-5 and TNU-9 were derived by expanding the HRTEM image along the direction perpendicular to it. However, density maps derived by using other approaches can also be used in FGDM, as long as structural information such as a framework channel system is clearly defined. For example, a structure envelope,

which can be generated by a Fourier transform from a small number of strong reflections with low indices, can be used.^[24] Such a structure envelope can define the pore system of a zeolite in real space, and has been shown to facilitate zeolite structure solution.^[25]

For the solutions of the highly complex framework structures of IM-5 and TNU-9, only the space group, the cell parameters, the number of T atoms, and one or two HRTEM images showing the pores were required. However, further information, such as structure factors from a diffraction experiment, can also be incorporated into the procedure. Preliminary tests show that this facilitates the convergence of the simulation. Our approach is simple, straightforward, and highly efficient. In this real-space modeling method, chemically reasonable bond lengths, bond angles, and connectivities for silicate framework structures have been embedded in the program code. However, given the corresponding bonding geometry information for open-framework materials with different chemical compositions and bonding connectivities, the method can easily be adapted to simulate their structures, too. Even nonporous materials could be addressed if suitable structural information can be derived from HRTEM images.

Received: November 9, 2007

Revised: January 30, 2008

Published online: April 24, 2008

Keywords: electron microscopy · microporous materials · molecular modeling · structure elucidation · zeolites

- [1] C. Baerlocher, L. B. McCusker, D. H. Olson, *Atlas of Zeolite Framework Types*, Elsevier, Amsterdam, **2007**.
- [2] A. W. Burton, *Z. Kristallogr.* **2004**, *219*, 866–880.
- [3] L. A. Bursill, E. A. Lodge, J. M. Thomas, *Nature* **1980**, *286*, 111–113.
- [4] P. Wagner, O. Terasaki, S. Ritsch, J. G. Nery, S. I. Zones, M. E. Davis, K. Hiraga, *J. Phys. Chem. B* **1999**, *103*, 8245–8250.
- [5] J. M. Thomas, O. Terasaki, P. L. Gai, W. Zhou, J. Gonzalez-Calbet, *Acc. Chem. Res.* **2001**, *34*, 583–594.
- [6] T. Ohsuna, Z. Liu, O. Terasaki, K. Hiraga, M. Cambor, *J. Phys. Chem. B* **2002**, *106*, 5673–5678.
- [7] D. L. Dorset, M. J. Roth, C. J. Gilmore, *Acta Crystallogr. Sect. A* **2005**, *61*, 516–527.
- [8] F. Gramm, C. Baerlocher, L. B. McCusker, S. J. Warrender, P. A. Wright, B. Han, S. B. Hong, Z. Liu, T. Ohsuna, O. Terasaki, *Nature* **2006**, *444*, 79–81.
- [9] C. Baerlocher, F. Gramm, L. Massüger, L. B. McCusker, Z. He, S. Hovmöller, X. Zou, *Science* **2007**, *315*, 1113–1116.
- [10] M. W. Deem, J. M. Newsam, *Nature* **1989**, *342*, 260–262.
- [11] J. Pannetier, J. Bassas-Alsina, J. Rodriguez-Carvajal, V. Caignaert, *Nature* **1990**, *346*, 343–345.
- [12] M. W. Deem, J. M. Newsam, *J. Am. Chem. Soc.* **1992**, *114*, 7189–7198.
- [13] M. Falcioni, M. W. Deem, *J. Chem. Phys.* **1999**, *110*, 1754–1766.
- [14] Y. Li, J. Yu, D. Liu, W. Yan, R. Xu, Y. Xu, *Chem. Mater.* **2003**, *15*, 2780–2785.
- [15] Y. Li, J. Yu, Z. Wang, J. Zhang, M. Guo, R. Xu, *Chem. Mater.* **2005**, *17*, 4399–4405.
- [16] S. W. Woodley, *Phys. Chem. Chem. Phys.* **2007**, *9*, 1070–1077.
- [17] E. Benazzi, J. L. Guth, L. Rouleau, *PCT Gazette*, WO 98/17581, **1998**.

- [18] S. Kirkpatrick, C. D. Gelatt, M. P. Vechi, *Science* **1983**, 220, 671–680.
 - [19] C. Baerlocher, A. Hepp, W. M. Meier, DLS-76, Distance Least Squares Refinement Program, Institut für Kristallographie, ETH Zürich, **1977**.
 - [20] W. M. Meier, H. J. Moeck, *J. Solid State Chem.* **1979**, 27, 349–355.
 - [21] T. Ohsuna, Z. Liu, O. Terasaki, K. Hiraga, M. A. Camblor, *J. Phys. Chem. B* **2002**, 106, 5673–5678.
 - [22] R. W. Grosse-Kunstleve, L. B. McCusker, C. Baerlocher, *J. Appl. Crystallogr.* **1997**, 30, 985–995.
 - [23] R. W. Grosse-Kunstleve, L. B. McCusker, C. Baerlocher, *J. Appl. Crystallogr.* **1999**, 32, 536–542.
 - [24] S. Brenner, L. B. McCusker, C. Baerlocher, *J. Appl. Crystallogr.* **1997**, 30, 1167–1172.
 - [25] S. Brenner, L. B. McCusker, C. Baerlocher, *J. Appl. Crystallogr.* **2002**, 35, 243–252.
-